

OPTIMUM DESIGN OF CANTILEVER WALLS RETAINING LINEAR ELASTIC BACKFILL BY USE OF GENETIC ALGORITHM

George Papazafeiropoulos, Vagelis Plevris, and Manolis Papadrakakis

National Technical University of Athens
Institute of Structural Analysis and Antiseismic Research
Zografou Campus, Athens 15780, Greece

gpapazafeiropoulos@yahoo.gr, {vplevris, mpapadra}@central.ntua.gr

Keywords: Genetic Algorithm, dynamic soil-structure interaction, linear elastic soil response, retaining wall.

Abstract. *Retaining walls are used in many geotechnical engineering applications, e.g. supporting deep excavations, bridge abutments, harbor-quay walls, anchored retaining walls, etc. Although they are generally simple structures, their static and dynamic interaction with the supporting and/or retained soil is a subject of ongoing research. Apart from this, seismic design of retaining walls is primarily based on rules of thumb and the designer's experience, in order to set the initial dimensions and make the necessary checks to comply with the design codes. In addition, the calculation of the seismic earth pressures is done in a rather simplistic way which may lead to either conservative or unsafe designs. In the present study, after a comprehensive literature review, optimum design is performed for cantilever walls retaining soil layers of two different heights, using numerical two-dimensional simulations and a genetic algorithm. Numerical simulations are performed using the finite element code ABAQUS [1] whereas for optimization purposes, the genetic algorithm provided with MATLAB [2] is utilized. For the calculation of the seismic earth pressures, linear elastic soil, retaining wall stem and wall foundation are assumed. The optimization procedure involves four design variables that have to do with the wall geometry, while the soil and wall material parameters and the frequency range of interest are kept fixed. Structural and geotechnical constraints as well as upper and lower bounds for the design variables are imposed to ensure technical feasibility of the solutions. The results on the optimum solutions are presented and comparisons are made with the corresponding results according to conventional seismic design methods. The numerical results of the study provide a clear indication of the direct dynamic interaction between the retaining wall and the surrounding soil, whereas the complexity of the optimization problem itself is evident. This justifies the necessity for a more elaborate consideration of the optimum design of retaining walls, especially if material and geometric non-linearities are taken into account.*

1 INTRODUCTION

Cantilever retaining walls are among the simplest and most common geotechnical structures intended to support earth backfills. Their main representatives are retaining walls supporting deep excavations, bridge abutments, harbor-quay walls, anchored retaining walls, etc. Their design must satisfy two major requirements: internal and external stability. The former ensures the structural integrity of the various parts of the retaining wall; the latter ensures that the wall – soil system formed after construction will remain in equilibrium, except for some displacements of affordable magnitude.

Retaining walls have to satisfy constraints imposed by the norms, assumptions, preferences and the target to be accomplished, and simultaneously have to be as economical as possible. The design is based on a trial-and-error procedure, which renders the experience of the designer an important factor to reach a cost-effective design. This manual research for the optimum design may be very time-consuming and tedious, while it is not ensured that the final result will be the optimum possible. This necessitates the need for application of various optimization procedures in order to achieve the optimum design.

Relevant optimization methods range from relatively simple mathematical programming based (exact) methods to novel heuristic search techniques. The methods belonging to the first category are very efficient for cases with a few design variables. Representative studies of this category are conducted in [3-6]. In [3] a design aid is compiled from results of an exhaustive search, with which simple rules of thumb were developed to provide for minimum cost design of cantilever retaining walls. In [4] optimization of reinforced concrete cantilever retaining walls is performed and the optimum design problem is posed as a constrained non-linear programming problem with seven design variables. Cost and weight of the walls were used as objective functions and overturning failure, sliding failure, no tension condition in the foundation base, shear and moment capacities of toe slab, heel slab, and stem of wall as constraints. In [5] the problem of optimal cost design of cantilever retaining walls is formulated as a non-linear programming problem and a sequential unconstrained minimization technique is adopted. In [6] optimum reliability-based design of cantilever retaining walls was presented by considering the parameter uncertainties and evaluating the safety in terms of reliability index and not merely by calculating the safety factor.

However, exact methods require large computational effort when the number of design variables increases, and apart from this, they require gradient information and seek to improve the solution in the neighborhood of a starting point. So, in order to attain an optimum design, one has to resort to more robust optimization techniques, which are capable of searching effectively the whole design variable domain and not being trapped into local optima. Recently developed heuristic methods, such as genetic algorithms, simulated annealing, threshold accepting, tabu search, ant colonies, particle swarm, etc. provide more attractive alternatives. Although these methods use simple algorithms, they require great computational effort. Representative studies of optimum design of retaining walls by use of heuristic methods are those presented in [7-16]. In [7] an application of a simulated annealing algorithm is reported to minimum cost design of reinforced concrete cantilever retaining walls that are required to resist a combination of earth and hydrostatic loading by using only geometric design variables, whereas in [8] simulated annealing for optimum design of RC cantilever retaining walls used in road construction is utilized, by using more design variables, effectively leading to more detailed simulations. In [9] and [10] a modified particle swarm optimization (MPSO) based on PSO with passive congregation is proposed, to find the optimum cost design of a cantilever RC retaining wall. In [11] an Ant Colony Optimization (ACO) algorithm is applied to arrive at optimal design of a RC retaining wall (designed as a gravity wall, i.e. structural integrity is

not taken into account while imposing the constraints). In [12] a bacterial foraging optimization algorithm is presented whereas harmony search based algorithms were proposed in [13]. In [14] a genetic algorithm is applied to reach minimum cost design of three types of retaining walls: cantilever retaining wall, counterfort retaining wall and retaining wall with relieving platforms. In [15] a random direction search complex method is applied and three heuristic algorithms (genetic algorithm, particle swarm optimization and simulated annealing) are used to obtain the minimum cost design of a reinforced concrete cantilever retaining wall. Finally, in [16] optimum design of gravity retaining walls subject to dynamic loading was performed using a charged system search algorithm, while the Mononobe-Okabe method was used to determine the dynamic earth pressures.

Common feature of all the aforementioned studies is the fact that for the design of the retaining wall, dynamic earth pressures are ignored (except for [16] in which they are taken into account in a simplistic way through a pseudostatic approach). In addition, the static earth pressures (resulting from gravity and/or surcharge load) are calculated according to Rankine or Coulomb earth pressure theories which assume that a state of plastic equilibrium is developed in the retained backfill. Moreover, to the authors' knowledge, no suitable constraint has been imposed to any retaining wall optimum design case to ensure that the deformations of the retaining wall and the backfill are within acceptable limits. In most studies, this is ensured implicitly by avoiding the possibility of overturning and sliding, by controlling the stresses within allowable limits and by securing the stability of the retaining wall – retained soil system.

Apart from these, the seismic response of retaining systems is still a matter of ongoing experimental, analytical and numerical research. The dynamic interaction between a wall and a retained soil layer makes the response complicated. The dynamic analysis becomes much more complex, as usually material and/or geometry non-linearities have to be taken into account [17, 18]. Depending on the expected material behavior of the retained soil and the possible mode of the wall displacement, there exist two main categories of analytical methods used in the design of retaining walls against earthquakes: (a) the pseudo-static limiting-equilibrium solutions which assume yielding walls resulting in plastic behavior of the retained soil [19-21], and (b) the elasticity-based solutions that regard the retained soil as a viscoelastic continuum [22-24]. In most studies presented so far, in order to perform optimum design of retaining walls, the assumption of pseudo-static limiting equilibrium is made; therefore the design is performed in a simplistic way, ignoring the possibility of a linear elastic or viscoelastic soil backfill.

This study is concerned with the optimum design of cantilever retaining walls which are subject to earthquake loading and are responding in a linear elastic way. The objective function which is optimized is the weight of the retaining wall. This is roughly proportional to its construction cost, as the latter is generally an increasing function of the weight of the material used. This function is minimized subject to design constraints. Apart from the usual constraints imposed in most optimization studies, in this study a direct design constraint is imposed which controls the rocking response of the retaining wall. The optimization analysis is conducted via the use of a genetic algorithm, since in [15] it is shown that GA can be successfully applied for the optimal solution of structural optimization problems with many design variables and complex constraints. Two numerical examples are presented, in which optimum designs are performed for two values of the height of the soil layer to be retained.

2 NUMERICAL MODELING

In this section the numerical model used to simulate the dynamic response of a cantilever retaining wall is described. This model consists of an infinite soil layer with horizontal base and

free surface which is at higher elevation towards $+\infty$ than $-\infty$. These two elevations result in the existence of a vertical slope of height H which is retained by a cantilever wall. The wall's foundation is at a depth equal to h_{emb} , relative to the downstream soil surface. Consequently, the overall height of the retaining wall stem is $H+h_{emb}$. The retaining wall is considered to rest on a strip foundation which consists of the toe, which is the portion of the foundation extending downstream from the wall, and of the heel, extending in the opposite direction (upstream). The depth of the rigid bedrock from the foundation of the wall is $1.5 \cdot H$, where H is the thickness of the horizontal layer to be retained, as seen schematically in Figure 1. The distance from the wall toe tip to the far field (downstream) vertical boundary of the model is $10 \cdot H$; the same happens with the distance from the wall heel tip to the far field boundary of the model in the upstream direction. Shown in Figure 1 is also the local coordinate system to which the graphs showing the internal forces and stress distributions along the wall or its components in later sections refer. Text in bold denotes the design variables whereas the others either denote the variables which are dependent on the design variables or are problem parameters which remain fixed during optimum design.

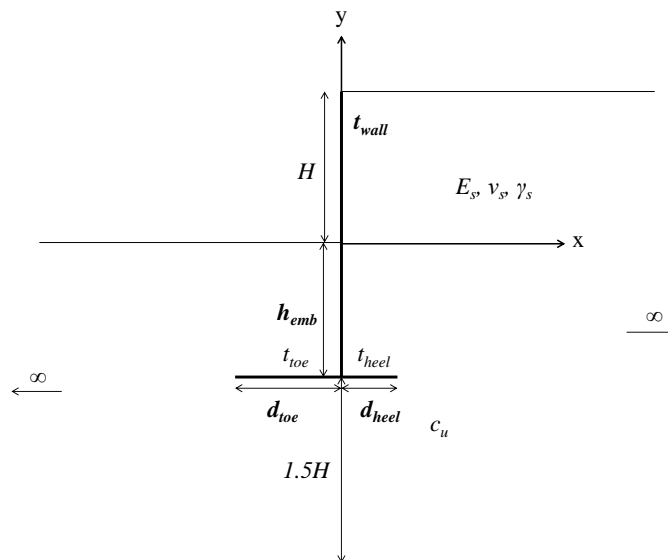


Figure 1: Cantilever reinforced concrete retaining wall model considered in this study.

The soil layer is fixed on rigid bedrock and along the soil – rock interface horizontal and vertical fixity is imposed. In order to simulate sufficiently the one dimensional dynamic soil response, vertical kinematic constraints were used at the two vertical ends of the model. These constraints are different from the corresponding kinematic constraints imposed for gravity loading at the same boundaries, which were in the horizontal direction to simulate one dimensional compression. The two vertical boundaries of the model were placed relatively far from the wall to minimize the influence of the difference between the model response in these regions and one dimensional soil response. The whole model is considered to respond in plane strain condition, an assumption fairly accurate for cantilever retaining walls with length much higher than their width, height and thickness. The wall – soil and the foundation – soil interfaces are considered to be tied, an assumption generally valid for cohesive soils. This means there is no separation or relative slip along these interfaces. Initially, gravity acceleration (body force) is applied to the whole model and in a second step of the analysis, the transverse ground acceleration record recorded during the December 11, 1967 Koyana earthquake, which

was of magnitude 6.5 on the Richter scale, is imposed along the base of the soil layer. The time history graph of this record is shown in Figure 2.

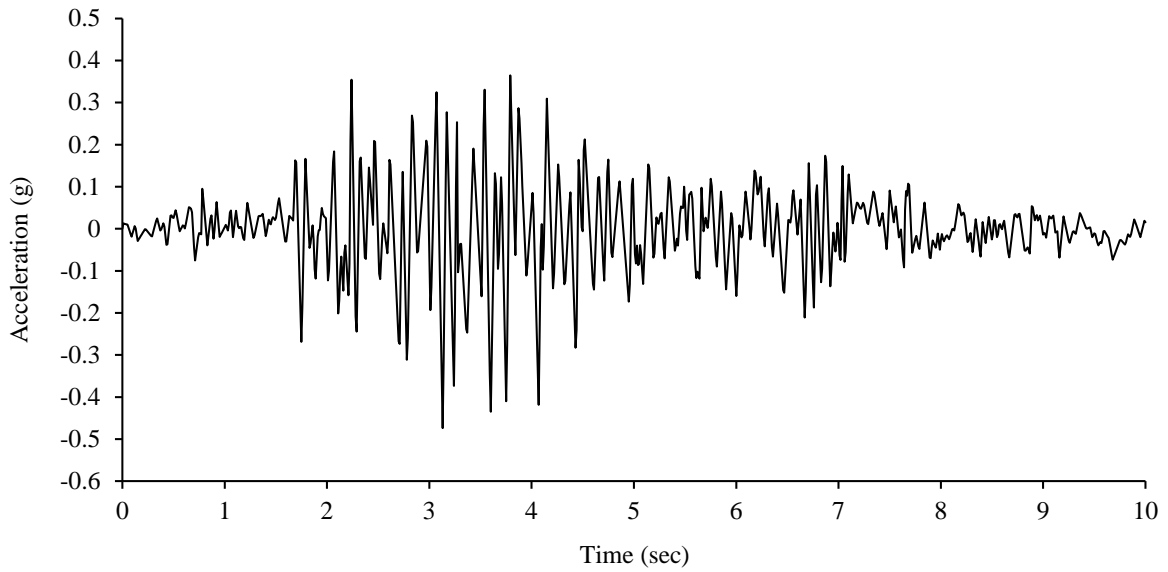


Figure 2: Transverse acceleration time history record of the December 11, 1967 Koyuna earthquake, of magnitude 6.5 on the Richter scale.

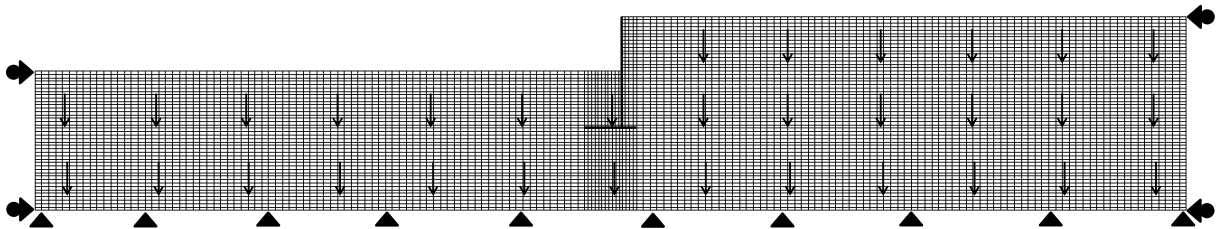


Figure 3: Numerical model analyzed for the 1st case (H=8m). Loading and boundary conditions for the initial gravity step are shown.

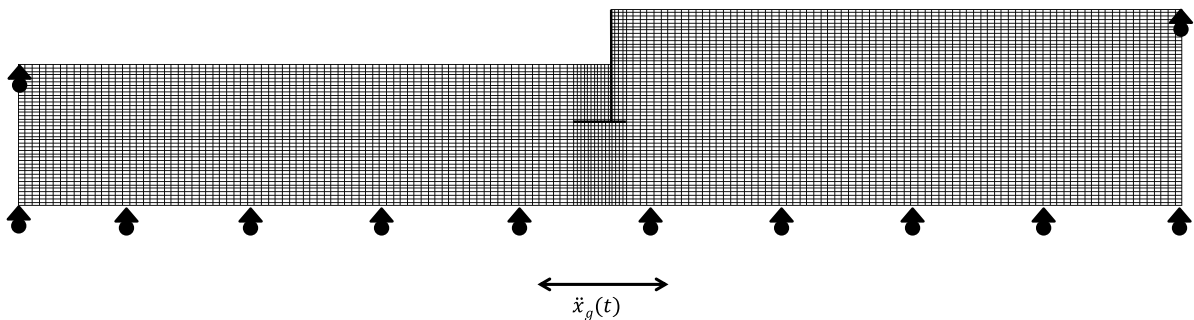


Figure 4: Numerical model analyzed for the 1st case (H=8m). Loading and boundary conditions for the main dynamic time – history analysis step are shown.

In this study, in order to minimize the weight of the retaining wall, two-dimensional numerical simulations were performed for the wall-soil systems depicted in Figures 3 and 4, utilizing the finite element software ABAQUS [1]. The soil layer is discretized with 8-node

biquadratic plane strain solid elements (CPE8). 3-node quadratic interpolation beam elements in plane (B22) are used for modeling the retaining wall and its foundation. These elements allow for transverse shear deformation according to Timoshenko theory and in their shear flexible formulation it is assumed that the transverse shear behavior is linear elastic with a fixed shear modulus and, thus, independent of the response of the beam section to axial stretch and bending. For Timoshenko beam elements a lumped mass formulation with a 1/6, 2/3, 1/6 distribution is used. The mesh gets coarser for the part of the soil layer which is left and right of the wall (the horizontal dimension of the elements is double). This is apparent in Figures 3 and 4.

The eigenmodes used for the modal dynamic analysis are extracted in a previous frequency step, in which the Lanczos eigensolver is used, which is a powerful tool for extraction of the extreme eigenvalues and the corresponding eigenvectors of a sparse symmetric generalized eigenproblem. For the Lanczos eigensolver, the minimum and maximum frequencies of interest are specified and all eigenmodes with eigenfrequencies falling in this range are extracted. These modes are subsequently used for the calculation of the dynamic response during the modal dynamic analysis. Energy dissipation due to damping mechanisms is not modeled explicitly as a material property (e.g. through the simplistic Rayleigh damping approximation), but it is specified as a fraction of critical damping assigned at all eigenmodes included for the calculation of the dynamic response, equal to 5%. Thus the damping fraction remains constant along the frequency range of interest and energy dissipation is of the same intensity for lower and higher frequencies.

3 FORMULATION OF THE OPTIMIZATION PROBLEM

In this section the optimization problem to be solved is explained in detail. The design variables, the parameters, the constraints, the objective function and the optimum design process are presented.

3.1 Design variables

The design variables of the problem are shown in bold in Figure 1. These are the depth of the wall embedment denoted by h_{emb} , the width of the toe denoted by d_{toe} , the width of the heel denoted by d_{heel} and the thickness of the wall stem denoted by t_{wall} . The thickness of the wall toe and heel (t_{toe} and t_{heel} respectively) are selected to be the same and equal to the minimum between the wall stem thickness t_{wall} and one tenth of the corresponding widths ($d_{toe}/10$ and $d_{heel}/10$), so that beam modeling for these components is reasonable.

Design variable	Lower limit (m)	Upper limit (m)
h_{emb}	0.2	16
d_{toe}	2	12
d_{heel}	2	12
t_{wall}	0.2	2.5

Table 1: Design variables of the optimization problem and their lower and upper bounds.

In the aforementioned design variables upper and lower limits are set, in order to prevent the algorithm from giving technically infeasible solutions. Table 1 shows the design variables and their corresponding upper and lower limits.

3.2 Parameters

The parameters of the wall-soil layer system are all the quantities that remain fixed during a particular optimization search. The parameters of the problem are summarized in Table 2. These are the physical properties of the soil and the wall. All materials involved in the model are linear elastic, leading thus to a linear dynamic response. The soil has density $\gamma_s=1800$ kg/m³, modulus of elasticity $E_s=100$ MPa and Poisson's ratio $\nu_s=0.3$. The retaining wall is modeled as a reinforced concrete beam with a general section, density $\gamma_w=2500$ kg/m³, and modulus of elasticity $E_w=30.5$ GPa which corresponds to C25/30. Although the retaining wall has the inertial and stiffness characteristics of concrete, it deforms in a linear elastic way, which implies that its stiffness in tension and compression is equal. Another parameter of the problem is the frequency range used for the modal dynamic analysis; this is selected to be in the range [0.01 Hz, 29 Hz]. The lower limit is selected so that the very low frequency spurious eigenmodes are excluded from the analysis; these are associated with very large modal mass. The higher limit is selected based upon the fact that the lowest wavelength of the waves propagating into the soil (lowest velocity of propagation and highest frequency) has to be at least ten times the internodal interval of the mesh; this is approximately the distance between adjacent nodes, and it increases as the mesh gets coarser.

Parameter	Assigned value
γ_s	1800 kg/m ³
E_s	100 MPa
ν_s	0.3
γ_w	2500 kg/m ³
E_w	30.5 GPa
f_{min}	0.01 Hz
f_{max}	29 Hz

Table 2: Parameters of the optimization problem and their fixed values.

3.3 Constraints

The constraints of the optimization problem at hand are divided into structural constraints and geotechnical constraints. The satisfaction of the former ensures that the retaining wall does not fail as regards its structural integrity, whereas the latter ensures that the soil retained by and supporting the wall does not fail. The constraints are shown in Table 3, which includes the formulas for the calculation of the limiting quantities and the constraint inequalities imposed for the optimization problem. As far as the structural constraints are concerned, the maximum tensile (and the minimum compressive) stress which develop due to axial force and bending moment at the wall stem, toe and heel must not be higher than (respectively lower than) the material strength. For concrete C25/30 this is 25 MPa by definition, without taking into account the partial safety factor for concrete strength [25]. The material model used for the wall in this study is linear elastic and this leads to the essential assumption that the distribution of strains and stresses along the section of the wall and its foundation is linear which results in the presence of "theoretical" tensile stresses which are not present in practice. In practice, there are no tensile concrete stresses and the necessary tensile forces for the equilibrium of the section are provided by the steel reinforcement. In any case, the tensile stress constraint is not active in the final optimum design, as will be described in detail later. Shear stiffness is ignored since shear strength of reinforced concrete cannot be calculated in a theoretically sound basis; the procedure of calculation and the final result is very norm specific in

general. Except for this, it depends highly on the reinforcement and its distribution into the beam. Concerning the geotechnical constraints, the following are specified:

a) It is ensured that the normalized displacement at the top of the wall stem θ does not exceed 0.33%. The normalized displacement is given by the ratio of the horizontal displacement at the top of the wall due to tilting or horizontal translation, divided by the height of its stem including embedded part ($H+h_{emb}$). The above inequality is specified to prevent the development of a limit state or the initiation of a failure plane in the retained soil [26]. In the opposite case the assumption of a linear elastic soil would not be accurate. It is assumed in this study that, as far as its strength is concerned, the supporting and retained soil behaves like compacted clay. According to [26] the values of normalized displacement required to reach active and passive earth pressure conditions are 1% and 5% respectively. By ensuring that the normalized displacement is lower than 0.33% (conventionally taken as one third of the normalized displacement required for active conditions) neither active nor passive states will develop in the soil.

Quantity	Formula	Constraint
Normalized displacement of wall stem	$\theta = \max[\text{abs}\{Displ_{top}/(H+h_{emb})\}]$	$\theta \leq 0.33\%$
Undrained shear strength	$c_u = E_u/850 = 3 \cdot E_s / \{2 \cdot (1 + \nu_s)\} / 850 = 136 \text{ kPa}$	$\max(\tau) \leq c_u$ $\min(\tau) \geq -c_u$
Soil bearing capacity	$q_u = 5.14c_u + \gamma_s \cdot h_{emb}$	$-\min(\sigma_{yy}) \leq q_u$
Foundation uplift		$\max(\sigma_{yy}) \leq 0$
Max bending stress*	$\sigma_{max} = \max(N/t + 6M/t^2)$	$\sigma_{max} \leq 25 \text{ MPa}$
Min bending stress*	$\sigma_{min} = \min(N/t - 6M/t^2)$	$\sigma_{min} \geq -25 \text{ MPa}$

* For the wall stem, toe and heel. t denotes t_{stem} , t_{toe} and t_{heel} .

Table 3: Constraints of the optimization problem.

b) Regarding its strength, the soil is assumed to behave as a cohesive soil in undrained conditions. So, its shear strength in terms of total stresses is equal to its undrained shear strength c_u , i.e. the $\phi=0$ approach is followed. Thus, it is specified that the maximum and minimum shear stress along the wall foundation must not exceed the undrained shear strength of the underlying soil, equal to 136 kPa. This value is calculated as follows: the undrained modulus of elasticity E_u of the soil is calculated according to Table 3 to be $E_u=115.38 \text{ MPa}$. The fraction E_u/c_u according to data available in the literature [27, 28], is selected to be roughly 850.

c) The bearing capacity of the soil underlying the foundation must not be surpassed. For this purpose, the bearing capacity under undrained loading ($c = c_u$, $\phi = 0$) is calculated according to the Meyerhof formula for vertical and central loading of horizontal strip foundation at a depth equal to h_{emb} . The maximum vertical normal stress at the lower interface of the wall foundation must not get larger than this value.

d) Along the interface where constraint (c) is imposed, there must also be no tension, otherwise there would be foundation uplift which would render the dynamic response of the retaining wall geometrically non-linear.

The approach followed to impose the constraints is the penalty method. Penalty methods add a penalty to the objective function to decrease the quality of infeasible solutions. The penalty quantities that are added are virtually the product of the constraint violation and a penalty factor which is fixed for each constraint and adjusted to take into account the relative importance of the constraint violations.

3.4 Objective function

The objective function to be minimized is the volume of the retaining wall per meter in the longitudinal direction. This is proportional to its weight and indirectly related to its cost of construction. The fitness function which is minimized by the genetic algorithm used in this study results from the objective function after the application of the penalties due to constraint violations, if any.

4 GENETIC ALGORITHM USED FOR OPTIMIZATION

The Genetic Algorithm (GA) is a stochastic global search optimization method that emulates natural biological evolution. GAs apply on a population of potential solutions the principle of survival of the fittest to produce better approximations to a solution. At each generation, a new set of approximations is created by the process of selecting individuals according to their level of fitness in the problem domain and breeding them together using operators borrowed from natural genetics (crossover, mutation, etc.). This process leads to the evolution of individuals that are better suited to their environment than the individuals that they were created from, just as in natural evolution process. In order to minimize the objective function, the genetic algorithm implemented in MATLAB software [2] was used.

The encoding strategy followed is real-valued representation. The use of real-valued genes in GAs offers a number of advantages in numerical function optimization over binary encodings: (a) efficiency of the GA is increased as there is no need to convert chromosomes to phenotypes before each function evaluation, (b) less memory is required as efficient floating point internal computer representations can be used directly, (c) there is no loss in precision by discretization to binary or other values and (d) there is greater freedom to use different genetic operators.

The population size (number of individuals in each generation) is equal to 20. The initial population with which the GA begins is created as a random initial population with uniform distribution. Fitness scaling was implemented by using a rank function, which scales the raw scores based on the rank of each individual instead of its score. The rank of an individual is its position in the sorted scores. An individual with rank r has scaled score proportional to $r^{-1/2}$. Rank fitness scaling removes the effect of the spread of the raw scores. The square root makes poorly ranked individuals more nearly equal in score, compared to rank scoring.

Regarding the basic genetic operators, stochastic uniform selection is used for the selection process. In this function each parent corresponds to a section of the line of length proportional to its scaled value. The algorithm moves along the line in steps of equal size. At each step, the algorithm allocates a parent from the section it lands on. The first step is a uniform random number less than the step size. For reproduction, the number of individuals that are guaranteed to survive to the next generation (elite children) is 2 and the fraction of the next generation, other than elite children, that is produced by crossover (crossover fraction) is equal to 0.8. The mutation function used is Gaussian, which adds a random number taken from a Gaussian distribution with mean 0 to each entry of the parent vector. For the combination of parents to produce the next generation offspring (crossover), scattered crossover is used, which applies in problems without linear constraints. It creates a random binary vector and selects the genes where the vector entry is 1 from the first parent, and the genes where the vector entry is 0 from the second parent, and combines the genes to form the child. In the GA no migration occurs, as there are no subpopulations.

As stopping criteria for the algorithm the following were specified: (a) the maximum number of iterations for the genetic algorithm to perform is equal to 100, (b) the algorithm stops if

the weighted average relative change in the best fitness function value over 50 generations is less than or equal to the function tolerance (equal to 10^{-6}).

The following outline summarizes how the GA procedure works:

- a) The algorithm begins by creating a random initial population.
- b) The algorithm then creates a sequence of new populations. At each step, the algorithm uses the individuals in the current generation to create the next population. To create the new population, the algorithm performs the following steps:
 1. Scores each member of the current population by computing its fitness value.
 2. Scales the raw fitness scores to convert them into a more usable range of values.
 3. Selects members, called parents, based on their fitness.
 4. Some of the individuals in the current population that have better fitness are chosen as elite. These elite individuals are passed to the next population.
 5. Produces offspring from the parents. Offspring are produced either by making random changes to a single parent (mutation) or by combining the vector entries of a pair of parents (crossover).
 6. Replaces the current population with the offspring to form the next generation.
- c) The algorithm stops when one of the stopping criteria is met.

The GA optimizer is properly coupled with the analysis solver in order to take the modal dynamic analysis results. This is done inside the objective function in which the analysis solver is called to perform the necessary analyses. Except for this, suitable functions are called to create the necessary input (*.inp) files to conduct the analyses and read the results of the analyses from the corresponding results (*.fil) files. While the analysis solver is running the optimizer is halted and its execution is continued after the lock (*.lck) file has been deleted. Constraint enforcement is applied through an advanced penalty method and not by the default constraint handlers developed in MATLAB.

5 CONVENTIONAL SEISMIC DESIGN OF CANTILEVER RETAINING WALLS

Conventional seismic design of cantilever reinforced concrete retaining walls is achieved with use of the well-known Mononobe-Okabe (M-O) theory of seismic earth pressures [19, 20]. Design is performed regarding the wall stability (sliding and overturning about the tip of its toe), and the design variables are the wall embedment (h_{emb}), the width of the wall toe (d_{toe}) and the width of the wall heel (d_{heel}). The thickness of the wall stem and foundation (toe and heel) are selected based on general guidelines for initial wall dimension proportioning, i.e. they are set equal to 1/10 of the total wall height ($H+h_{emb}$). According to the dimension proportioning practice, the inequality $0.3 \cdot (H+h_{emb}) \leq d_{heel} \leq 0.5 \cdot (H+h_{emb})$ must hold for the width of the wall heel. The minimum values of the wall embedment, toe width and heel width are set equal to 0.2 m, 2 m and 2 m respectively. The conventional seismic design method implemented in this study involves also some kind of optimization procedure which leads to the minimum total weight of the wall by strict abidance by all of the constraints mentioned above.

A necessary step during the design process is the evaluation of the soil internal friction angle φ and the soil – wall interface friction angle δ . These are set to the following typical values: $\varphi=30^\circ$, $\delta=18^\circ$. The horizontal acceleration coefficient is taken as $k_h=0.48$ (resulting from the maximum acceleration of the earthquake record which is 0.48g). These properties are assigned to the soil lying over the wall foundation. For the soil under the wall foundation undrained response is assumed, namely its internal friction angle is taken equal to zero and its undrained shear strength c_u is the one specified in section 3 of this study. The inertial forces and moments of the wall are also taken into account for the design whereas, regarding overturning checks, only the upstream and downstream soil portions lying over the wall foundation are considered to contribute to the wall stability.

6 NUMERICAL RESULTS

Two retaining wall weight optimization cases were examined in this study: in the first case (Case 1) the height of the soil layer to be retained by the wall is equal to 8 m and in the second case (Case 2) the height is 12 m. The results of the GA optimization procedure as analyzed in the previous sections are shown in Table 4. It is observed in general that the embedment and foundation dimensions required to retain the soil layer with greater height (Case 2) are larger than those in Case 1. The optimum value of the objective function increases as well. In both cases, the length of the wall heel (d_{heel}) which leads to optimum design is the minimum possible, i.e. its lower bound. This means that for the parameter values and earthquake record considered in this study the heel does not contribute significantly to the retaining wall stability and/or structural integrity. The thickness of the heel is constrained by the requirement that it is not more than one tenth of its length (to justify its modeling as a beam), whereas the thicknesses of the other components (stem and toe) are equal.

	Case 1 ($H=8m$)	Case 2 ($H=12m$)
Design variables		
h_{emb} (m)	7.76	7.16
d_{toe} (m)	4.57	6.57
d_{heel} (m)	2.00	2.00
t_{wall} (m)	0.20	0.22
t_{toe} (m)	0.20	0.22
t_{heel} (m)	0.20	0.20
Constraint quantities		
θ	0.328%	0.246%
$\max\tau$ (kPa)	78.42	88.46
$\min\tau$ (kPa)	-131.96	-135.73
$\min\sigma_{yy}$ (kPa)	-505.98	-592.45
$\max\sigma_{yy}$ (kPa)	-122.07	-124.53
$\sigma_{b,s,max}$ (kPa)	22570.73	21476.85
$\sigma_{b,t,max}$ (kPa)	4265.33	1183.35
$\sigma_{b,h,max}$ (kPa)	2029.97	2180.68
$\sigma_{b,s,min}$ (kPa)	-23795.84	-23385.15
$\sigma_{b,t,min}$ (kPa)	-7336.37	-8128.82
$\sigma_{b,h,min}$ (kPa)	-2176.36	-2501.06
Algorithm details		
Min. value of obj. fun. (m^2)	4.47	6.12
Number of generations	73	64
Number of fun. evaluations	1480	1300

Table 4: Results of the optimization procedure of the two retaining wall cases considered in this study.

Table 5 shows the results of the conventional seismic design according to the M-O method. It is observed that the conventional design which is adopted in most seismic norms worldwide leads to larger weight of the retaining wall. Although the two methods stem from essentially different assumptions, their comparison shows clearly the fact that more economical and simultaneously safe designs can be achieved by applying detailed optimization methods for the seismic design of retaining walls; current seismic code practices can lead to unreasonably conservative designs.

	Case 1 ($H=8\text{m}$)	Case 2 ($H=12\text{m}$)
h_{emb} (m)	0.20	0.20
d_{toe} (m)	5.58	8.43
d_{heel} (m)	4.10	6.10
t_{wall} (m)	0.73	1.32
t_{toe} (m)	0.73	1.32
t_{heel} (m)	0.73	1.32
Area (m^2)	13.05	35.28

Table 5: Results of the conventional seismic design of the two retaining wall cases considered in this study.

As far as the constraints are concerned, the maximum and minimum normal stresses of the heels of the two walls do not differ much. On the contrary, the maximum normal stress of the toe differs by a factor greater than 2 between the two wall cases. Furthermore, the minimum shear stress along the lower interface between the wall foundation and the supporting soil is roughly the same for the two wall cases. This observation implies that minimum shear stress along the lower interface of the wall foundation is independent of the wall height. Furthermore, the constraint imposed for this quantity is active in Case 2. The above may provide a hint for controlling the optimization process. To investigate more thoroughly the dynamic response of the retaining wall and the surrounding soil, the internal forces of the wall and the shear stress distributions along the wall foundation – soil lower interface are shown in the following sections.

7 DYNAMIC RESPONSE OF THE RETAINING WALL

In this section the dynamic response of the retaining wall in the two cases examined in this study is considered. Internal force distributions as well as normalized displacement at the wall top are presented. In Figure 5 the axial force distribution along the stem of the wall (including embedment) is shown for the case 1. This distribution refers to its optimum design with design variable values set as shown in case 1 of the previous section. The vertical axis (y) is associated with the Cartesian coordinate system shown in Figure 1. At the elevation of the downstream soil surface the y axis becomes zero, namely the horizontal axis of the diagrams coincides with the aforementioned soil surface. The two curves shown in Figure 5 show the maximum and minimum values respectively for each point of the wall stem. The two distributions presented do not occur in a specific instance during the earthquake loading; they are rather the two envelope curves which incorporate all the axial force distributions which occur over the whole time history during the dynamic response. The respective axial force distribution for the second case ($H=12\text{ m}$) is shown in Figure 6. It is apparent that the retaining wall

in both cases is subject to compression, which originates primarily from the gravity loading. In addition, the two envelope distributions have the same configuration, which advocates over this observation.

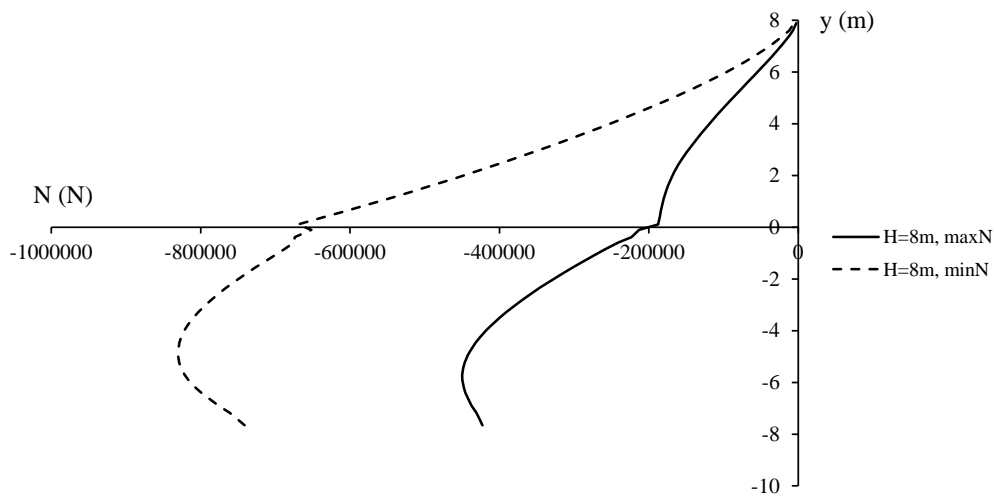


Figure 5: Maximum and minimum axial force distributions along the retaining wall stem for case 1 (H=8m).

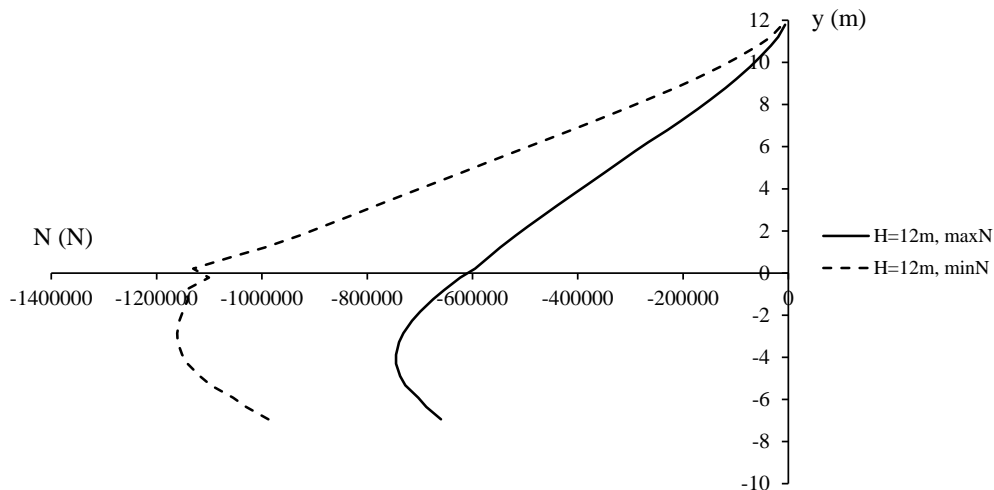


Figure 6: Maximum and minimum axial force distributions along the retaining wall stem for Case 2 (H=12m).

In Figure 7 and Figure 8 the maximum and minimum shear force distributions are shown for cases 1 (H=8m) and 2 (H=12m) respectively. It is observed that in case 1 the minimum and maximum distributions are approximately symmetric about the vertical axis (the stem of the wall). Since the fundamental eigenfrequencies of the upstream and downstream soil layers in case 1 are essentially higher than those in Case 2 (due to the fact that the layer thickness in case 1 is smaller than that in Case 2), it is more possible that the eigenfrequencies of the wall – soil system in case 1 lie within the dominant frequency range of the earthquake record. Thus, it is anticipated that the system of case 1 will exhibit more pronounced dynamic response, which stems from its kinematic and inertial dynamic interaction. Thus the rough symmetry between the two graphs is explained. On the contrary, in Case 2, where the eigenfrequencies are lower, the wall – soil system response is inertial for its most part, due to the lower frequency content. This result can be drawn also from the configuration of the shear force distri-

butions; they are positive near the surface of the downstream soil layer, become negative for lower elevation and get again positive at the foundation. This shows a quasi-static response.

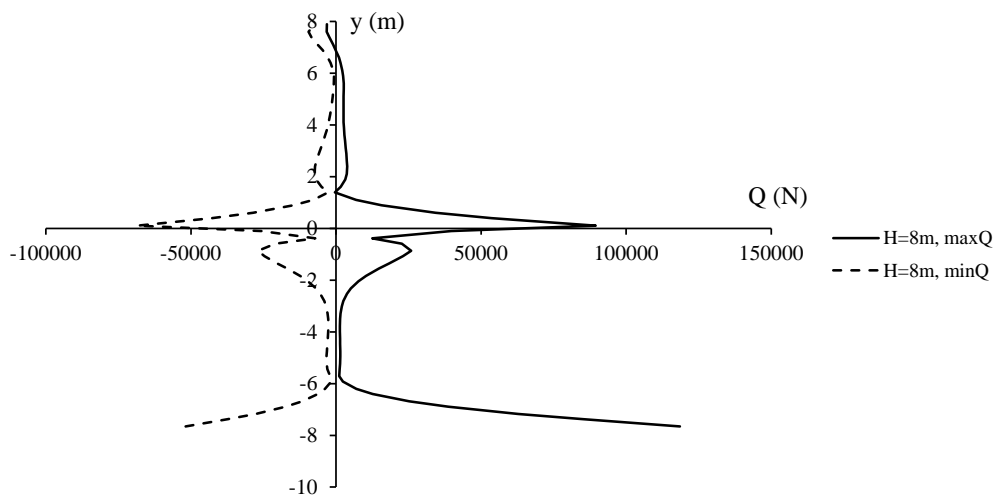


Figure 7: Maximum and minimum shear force distributions along the retaining wall stem for case 1 (H=8m).

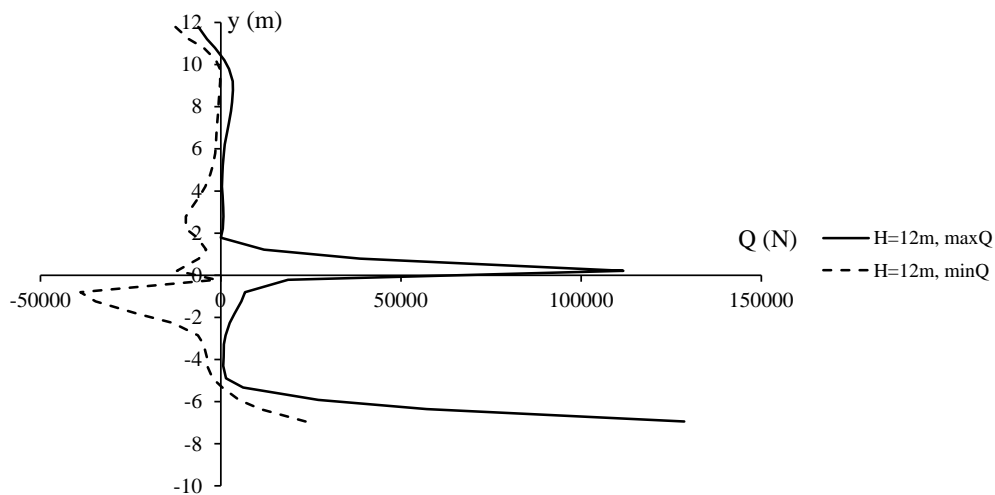


Figure 8: Maximum and minimum shear force distributions along the retaining wall stem for Case 2 (H=12m).

In both Figures 7 and 8 the shear force distributions display some common characteristics. They take local maxima (in terms of absolute values) at the wall foundation and at the surface of the downstream soil layer. The reason for the occurrence of the local maximum at the downstream soil layer surface is apparent; there is the point where passive soil pressures start, virtually relieving the distress due to soil pressures from the upstream soil layer. In the lower part of the wall stem shear forces from the foundation are transmitted. At the upper part of the wall shear forces are much lower and they depend highly on the wall compliance.

In Figures 9 and 10 the maximum and minimum bending moment distributions are shown for cases 1 ($H=8\text{m}$) and 2 ($H=12\text{m}$) respectively. Similar trends with the corresponding shear force diagrams are observed, i.e. the pronounced response of the wall in case 1 and the quasi-static response noted in Case 2. Along the part of the wall stem lying over its embedded part bending moments are mainly positive, as this part of the wall essentially retains the upstream soil layer. Bending moments show local optima at the same positions with the local optima of shear forces.

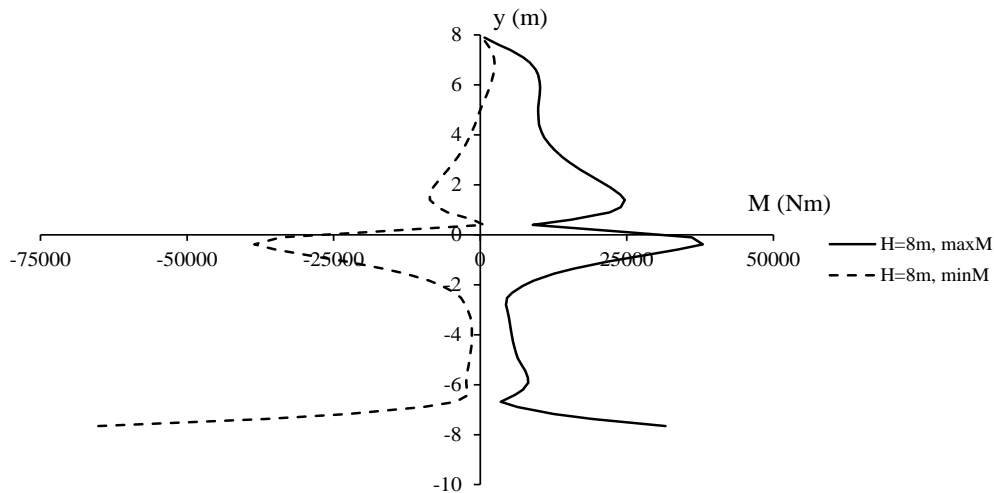


Figure 9: Maximum and minimum bending moment distributions along the retaining wall stem for case 1 ($H=8\text{m}$).

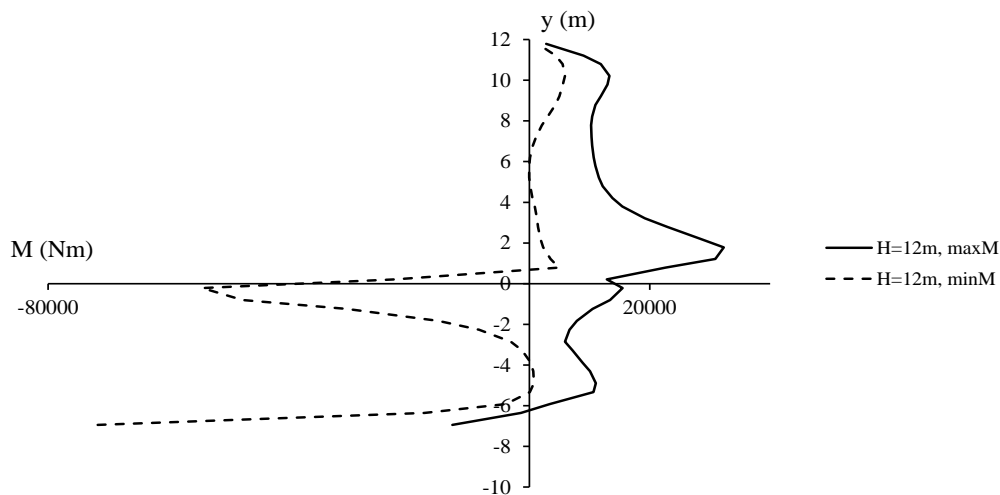


Figure 10: Maximum and minimum bending moment distributions along the retaining wall stem for Case 2 ($H=12\text{m}$).

In Figure 11 the variation in time history of the normalized displacement at the wall top is shown for cases 1 ($H=8\text{ m}$) and 2 ($H=12\text{ m}$). Firstly, it is noted that the dynamic response of the wall in the 1st case ($H=8\text{ m}$) is more pronounced than that in Case 2 ($H=12\text{ m}$). This agrees with the explanation given previously to interpret the dynamic nature of the response in case 1. However, although the maximum normalized displacement occurs for the 1st case, this does not entail that the response for this case is larger than that in Case 2 for the whole time history. Another observation to be made is that in case 1 the constraint affecting the

normalized displacement at the top of the retaining wall is active, i.e. controls the optimization process. This is expected, since the pronounced dynamic response in Case 1 leads to increased normalized displacement which eventually after the constraint imposition controls the optimization process.

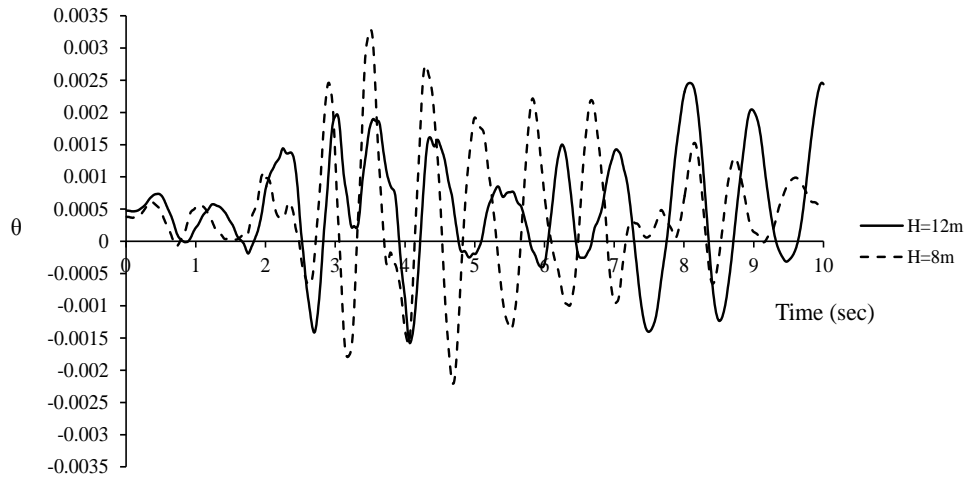


Figure 11: Normalized displacement at the top of the retaining wall for both cases considered in this study.

8 DYNAMIC SHEAR DISTRESS OF SUPPORTING SOIL

In this section the dynamic distress of the soil supporting the retaining wall is presented in terms of shear stresses. Especially, since shear stress is the primary factor affecting the stiffness and strength exhibited by soils in general, this quantity will be investigated. The region of the soil supporting the wall foundation which experiences the most intense shear stress is its interface with the lower horizontal boundary of the wall toe and heel. Plots of shear stress distributions developed along the wall foundation are shown in Figures 12 and 13 for the two cases examined in this study.

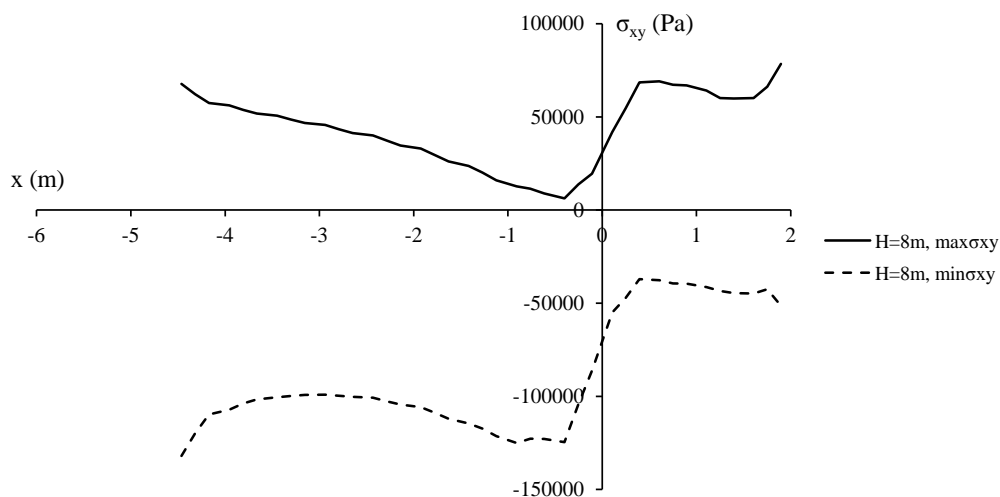


Figure 12: Maximum and minimum shear stress distributions along the retaining wall foundation (toe & heel) for case 1 (H=8m).

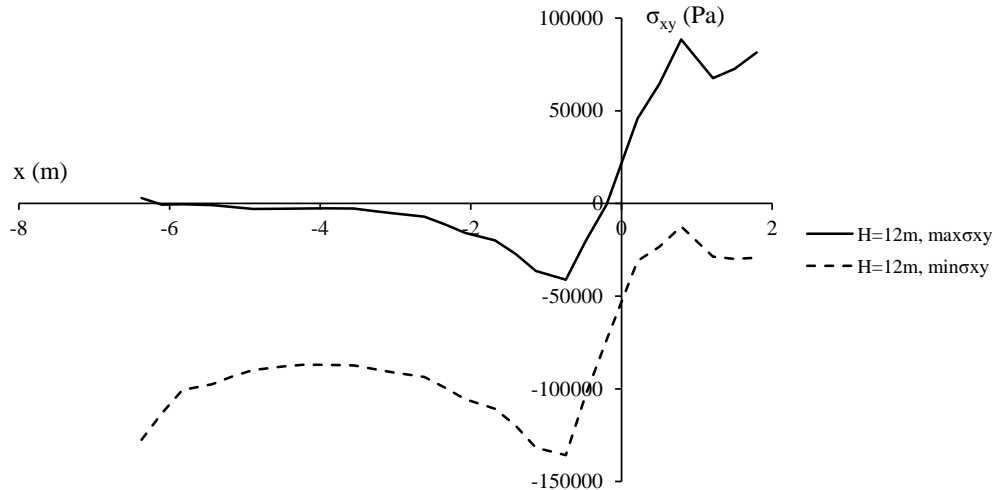


Figure 13: Maximum and minimum shear stress distributions along the retaining wall foundation (toe & heel) for Case 2 ($H=12\text{m}$).

The horizontal axis of these diagrams coincides with the wall foundation: its negative part shows the distribution along the wall toe and its positive part shows the distribution along the wall heel. Therefore, the vertical axis is in the same way coincident with the retaining wall stem. Its substantial difference from the horizontal axis is that it does not show vertical distance along the wall stem.

A major difference noted by comparing the two figures is that in Case 1 shear stresses may be positive (occurring when the retaining wall foundation is displaced towards the upstream soil layer) or negative (occurring when the retaining wall foundation is displaced towards the downstream soil layer). On the contrary, in Case 2, shear stresses along the wall toe are for the most part negative (since the distribution of the maximum shear stresses lies very close to the horizontal axis). This observation can be used as a hint to govern the optimization process. In both figures, along the wall heel the shear stress range tends to be generally higher than that along the wall toe.

9 CONCLUSIONS

- Unlike most optimization studies regarding retaining wall optimum design, two major features are examined in this study, i.e. optimum design for (a) seismic loading implemented through modal dynamic analysis with a rigorous time history integration procedure and (b) retaining wall – soil system responding linearly elastically.
- From the values of the design variables leading to retaining wall weight minimization it can be inferred that the length of the wall heel does not affect much its stability.
- Soil layers with increased thickness (and the same shear modulus and density) lead to systems with decreased eigenfrequencies. As a result, there is a greater possibility that their response to specific seismic loading is of more quasi-static nature, as is the 2nd case examined in the present study. The opposite happens with soil layers with decreased thickness; they show: (a) more pronounced dynamic response and (b) upper and lower internal force envelopes which tend to be more “symmetric”.
- For systems with increased dynamic response (such as Case 1 of this study) the constraints which control displacements (or their derivatives) are more likely to be active

during the optimization process, whereas for systems with quasi – static response (such as Case 2 of this study) the constraint controlling the shear stress along the wall foundation – supporting soil interface is more likely to be active.

- As far as the soil shear distress is concerned, in the quasi-static case ($H=12$ m) it is generally negative under the retaining wall toe.
- Conventional seismic design methods (M-O), even if they are applied in an optimal way, can lead to conservative designs by increasing the required material compared with more refined design methods such as the optimum design implemented in this study.
- Last but not least, it has to be mentioned that the genetic algorithm used for the optimization process in this study is efficient and robust, since it leads to the optimum solutions with a relatively low number of function evaluations and not being trapped in local minima.

REFERENCES

- [1] ABAQUS, *Analysis User's Manual Version 6.11*, Dassault Systèmes Simulia Corp., Providence, Rhode Island, USA.
- [2] MATLAB, *Global Optimization Toolbox Version 8 (R2012b)*, The MathWorks Inc., Natick, MA, USA.
- [3] E.J. Rhomberg, W.M. Street, Optimal design of retaining walls. *Journal of Structural Division, ASCE*, **107**, 992-1002, 1981.
- [4] A. Saribas, F. Erbatur, Optimization and sensitivity of retaining structures. *ASCE Journal of Geotechnical Engineering*, **122(8)**, 649–656, 1996.
- [5] P.K. Basudhar, B. Lakshman, A. Dey, Optimal cost design of cantilever retaining walls. *IGC 2006*, Chennai, India, December 14-16, 2006.
- [6] G.L. Sivakumar Babu, B. Munwar Basha, Optimum design of cantilever retaining walls using target reliability approach. *International Journal of Geomechanics, ASCE*, **8(4)**, 240-252, 2008.
- [7] B. Ceranic, C. Fryer, R.W. Baines, An application of simulated annealing to the optimum design of reinforced concrete retaining structures. *Computers and Structures*, **79**, 1569–1581, 2001.
- [8] V. Yepes, J. Alcalá, C. Perea and F. González-Vidosá, A parametric study of optimum earth retaining walls by simulated annealing. *Engineering Structures*, **30(3)**, 821-830, 2008.
- [9] M. Khajehzadeh, M. Raihan Taha, A. El-Shafie, M. Eslami, Economic Design of Retaining Wall Using Particle Swarm Optimization with Passive Congregation. *Australian Journal of Basic and Applied Sciences*, **4(11)**, 5500-5507, 2010.
- [10] M. Khajehzadeh, M. Raihan Taha, A. El-Shafie, M. Eslami, Modified particle swarm optimization for optimum design of spread footing and retaining wall. *Journal of Zhejiang University-SCIENCE A (Applied Physics & Engineering)*, **12(6)**, 415-427, 2011.

- [11] M. Ghazavi, S. Bazzazian Bonab, Optimization of Reinforced Concrete Retaining Walls Using Ant Colony Method. *3rd International Symposium on Geotechnical Safety and Risk (ISGSR)*, 2011.
- [12] M. Ghazavi, V. Salavati, Sensitivity analysis and design of reinforced concrete cantilever retaining walls using bacterial foraging optimization algorithm. *3rd International Symposium on Geotechnical Safety and Risk (ISGSR)*, 2011.
- [13] A. Kaveh, A.S.M. Abadi, Harmony Search Based Algorithm for the Optimum Cost Design of Reinforced Concrete Cantilever Retaining Walls. *International Journal of Civil Engineering*, **4(8)**, 336-357, 2010.
- [14] S. Donkada, D. Menon, Optimal design of reinforced concrete retaining walls. *The Indian Concrete Journal*, 9-18, 2012.
- [15] Y. Pei, Y. Xia, Design of Reinforced Cantilever Retaining Walls using Heuristic Optimization Algorithms. *2012 International Conference on Structural Computation and Geotechnical Mechanics, Procedia Earth and Planetary Science* **5**, 32 – 36, 2012.
- [16] S. Talatahari, R. Sheikholeslami, M. Shadfaran, M. Pourbaba, Optimum Design of Gravity Retaining Walls Using Charged System Search Algorithm. *Mathematical Problems in Engineering*, Vol. 2012, Article ID 301628.
- [17] S. Kramer, *Geotechnical Earthquake Engineering*, Prentice Hall, 1996.
- [18] G. Wu, W.D.L. Finn, Seismic lateral pressures for design of rigid walls. *Canadian Geotechnical Journal*, **36(3)**, 509-522, 1999.
- [19] S. Okabe, General theory of earth pressures. *Journal of the Japan Society of Civil Engineering*, **12(1)**, 1926.
- [20] N. Mononobe, H. Matsuo, On the determination of earth pressures during earthquakes. *Proceedings of the World Engineering Congress*, Tokyo, Japan, Vol. 9, Paper 388, 1929.
- [21] H.B. Seed, R.V. Whitman, Design of earth retaining structures for dynamic loads. *Proceedings of the ASCE Special Conference on Lateral Stresses in the Ground and Design of Earth Retaining Structures*, 103–147, 1970.
- [22] A.S. Veletsos, A.H. Younan, Dynamic Response of Cantilever Retaining Walls. *ASCE Journal of Geotechnical and Geoenvironmental Engineering*, **123(2)**, 161–172, 1997.
- [23] R.F. Scott, Earthquake induced pressures on retaining walls. *Proceedings of the 5th World Conference on Earthquake Engineering*, **2**, 1611–1620, 1973.
- [24] J.H. Wood, Earthquake – Induced Pressures on a Rigid Wall Structure. *Bulletin of New Zealand National Earthquake Engineering*, **8**, 175–186, 1975.
- [25] EC2, Eurocode 2: Design of concrete structures - Part 1-1: General rules and rules for buildings. *European standard CEN-EN-1992-1*, European Committee for Standardization, Brussels, 2004.
- [26] G.W. Clough, J.M. Duncan, Earth pressures. *Foundation Engineering Handbook*, ed. H-Y. Fang, 224–235, Van Nostrand Reinhold, New York, 1991.
- [27] M. Jamiolkowki, R. Lancellotta, S. Marchetti, R. Nova, E. Pasqualini, Design Parameters for Soft Clays. *Proc. 7th Eur. Conf. on Soil Mech. Found. Engrg.*, **5**, 21-54, Brighton, 1979.

- [28] R.J. Jardine, N.J. Brooks, P.R. Smith, The use of electrolevel gauges in triaxial tests on weak rock. *Int. J. Rock Mech. Min. Sci. and Geomech.*, **22(5)**, 331-337, 1985.